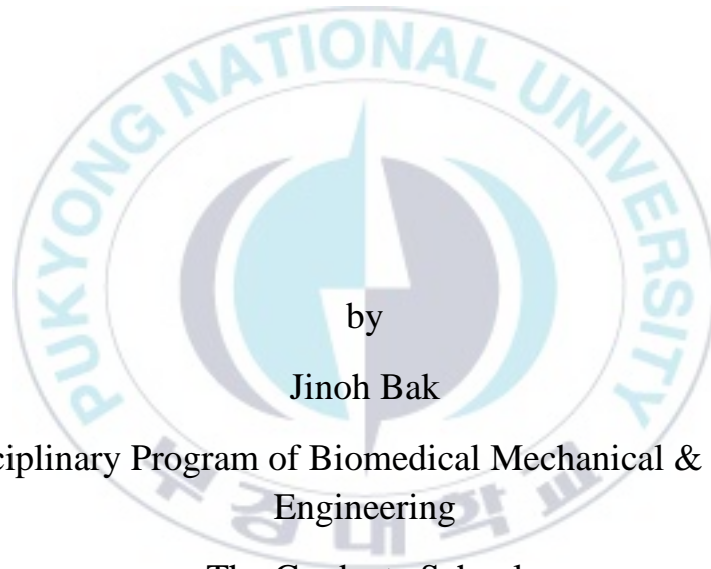


Thesis for the Degree of Master of Engineering

**Minimally invasive photothermal treatment
for benign stricture of gasto-intestinal tract
by balloon catheter integrated with optical
diffusing applicator**



by

Jinoh Bak

Interdisciplinary Program of Biomedical Mechanical & Electrical
Engineering

The Graduate School

Pukyong National University

January, 2019

**Minimally invasive photothermal treatment
for benign stricture of gastro-intestinal tract
by balloon catheter integrated with optical
diffusing applicator**

산광형 광섬유 융합형 풍선 카테터를
통한 양성 소화기관 협착의 최소 침습적
광열치료 연구

Advisor: Prof. Hyun Wook Kang

by

Jinoh Bak

A thesis submitted in partial fulfillment of the requirements
for the degree of

Master of Engineering in Department of Spatial Information Engineering,
The Graduate School,
Pukyong National University

January, 2019

Minimally invasive photothermal treatment for benign stricture of
gasto-intestinal tract by balloon catheter integrated with optical
diffusing applicator

A dissertation

by

Jinoh Bak

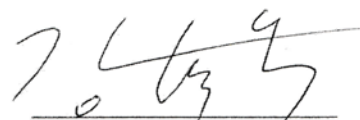
Approved by:



(Chairman) Junghwan Oh Ph. D



(Member) Sung-Won Kim M. D



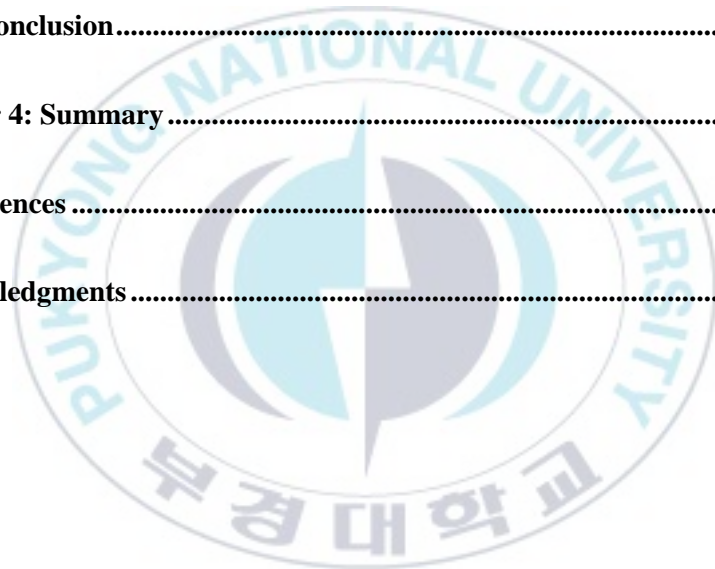
(Member) Hyun Wook Kang Ph. D

January, 2019

Table of Contents

Table of Contents	1
List of Figures	3
Abstract	5
Chapter 1: Introduction	1
1.1 Motivation	1
1.2 Thesis contribution	2
1.3 Concept of device	2
Chapter 2: Integration of optical applicator with balloon catheter for photothermal treatment of biliary stricture	4
2.1 Abstract	4
2.2 Introduction	5
2.3 Materials and Methods	8
2.5 Discussion	16
2.6 Conclusion	20
Chapter 3: Temperature-monitored optical treatment for radial tissue expansion	21

3.1 Abstract	21
3.2 Introduction	23
3.3 Method and Materials	25
3.4 Results	30
3.5 Discussion	36
3.6 Conclusion	40
Chapter 4: Summary	41
References	42
Acknowledgments	46



List of Figures

Chapter 1:

Figure 1. 1. Principle of balloon catheter integrated with optical diffusing applicator.	2
--	---

Chapter 2:

Figure 2. 1. Images of fabricated diffusing applicator for tissue testing: (a) micro-machined surface, (b) glass-capped fiber tip, and (c) balloon catheter-integrated diffuser.	8
Figure 2. 2. Experimental set-up of balloon catheter-assisted photocoagulation.....	10
Figure 2. 3. Thermal imaging on <i>ex vivo</i> porcine tissue during photocoagulation at 20 W: (a) IR image captured at 60 s after irradiation and (b) temporal development of temperature at various points of 0, 2.5, and 5 mm from proximal end of diffusing tip (P = proximal and D = distal ends; $N = 3$).....	12
Figure 2. 4. Spatial light distribution of diffusing applicator: (a) polar light emission (0.96 ± 0.02) and (b) temperature measured 60 s after laser irradiation and normalized longitudinal intensity at various fiber points (0 mm = proximal end and 5 mm = distal end; $N = 3$)	13

Figure 2. 5. Comparison of porcine bile ducts: (a) control, (b) treated tissue and (c) quantitative comparison of cross-sectional area variations between pre- and post-treatments ($N = 5$). 14

Figure 2. 6. Histological comparison ($\times 40$) after 20-W photocoagulation for 60 s: (a) control and (b) treated tissue stained by H&E.

Chapter 3:

Figure 3. 1. (a) Experimental set-up for *ex vivo* laser photocoagulation assisted with temperature monitoring and normalized spatial light distribution based on goniometer measurements: (b) 3D emission profile along diffuser and (c) polar light emissions from middle. 26

Figure 3. 2. Top-view images of tissues treated for (a) 5 s and (b) 30 s and corresponding thermal IR images acquired at (c) 5 s and (d) 30 s irradiation. 30

Figure 3. 3. Temporal development of temperature as function of irradiation time measured by thermocouple ($N=5$) and synchronized IR image by thermal camera. ... 32

Figure 3. 4. (a) Histology images after 10-W photocoagulation for (i) 10 s and (ii) 60 s ($\times 125$) and (b) luminal deformation in tissue after 10-W photocoagulation for various irradiation times (5, 10, 20, 30, 60, and 120 s) 33

Figure 3. 5. Variations in coagulation depth (black circle; left axis) and area expansion index (AEI, red circle; right axis) as function of irradiation time ($N = 5$; C.D. = coagulation depth, A_i = initial lumen area, and A_f = final lumen area). 34

**Minimally invasive photothermal treatment for benign stricture of gastro-intestinal tract
by balloon catheter integrated with optical diffusing applicator**

Jinoh Bak

Interdisciplinary Program of Biomedical Mechanical & Electrical Engineering

The Graduate School

Pukyong National University

Abstract

소화기관 협착은 일반적으로 삶의 질을 저하시키고 심하게는 사망에 이르기에도 할 수 있는 질병이다. 식도 협착은 위식도 역류질환 환자의 23 % 가 경험한다. 담관 협착은 위장관 질병의 수술 후 외상으로 인해 드물게 발생한다. 그러나, 위장관 협착증에 적용되는 현재의 치료법은 풍선 확장술, 스텐트 삽입술, 부유지 확장술 등 물리적인 확장에 의존하여 47 % 이상의 환자가 재협착 및 스텐트 밀림현상 같은 재수술을 필요로 한다. 최근 위장관 협착 치료에 광열치료가 촉망되는 협착 치료의 하나로 여겨지고 있다. 광열치료란 병변에 적합한 파장의 레이저를 조사해서 열 반응을 유도하고 상승한 온도로 협착에 열 응고를 발생시켜 영구적인 조직 변형을 유도하는 방법이다. 본 연구에서는 기존의 물리적 협착 지름 확장법과 광열치료법을 융합하여 물리적인 확장을 유도한 후 광열반응을 통해 영구적인 조직변형을 발생시키는 의료기기를 개발하고 실제 임상치료법으로서 가능성을 조사하였다. 기존의 풍선카테터의 원형에 산광형 광섬유를 결합하여 장비를 제작하였다. 병변 외의 조직에 원치 않는 열 손상을 최소화 하기 위해 실시간 온도 모니터링 광열치료 기법을 확인하였다. 실제 내시경 시술에 적용하기 위하여 장비의 내구도 및 과도한 물리적 변형에도 풍선 확장과 에너지 전달이 가능한지를 돼지 담관에 적합한 크기의 장비를 제작하여 동물 실험을 통해 담관 확장술로 효과를 조사하였다. 결과적으로 산광형

광섬유 융합형 풍선 카테터의 개발의 이러한 응용 및 접근은 효과적으로 소화기관 협착을 치료할 수 있는 방법이 될 수 있다. 추후 임상 적용을 위해서 추가적인 동물 실험과 융합형 전달기기의 내구도 및 전달력을 증대시키는 설계 및 연구가 이루어져야 할 것으로 여겨진다.



Chapter 1: Introduction

1.1 Motivation

The human digestive system consists of the gastrointestinal tract plus the accessory organs of digestion (the tongue, salivary glands, pancreas, liver, and gallbladder). Most of them are tubular tissue. These tubular tissues are easily exposed to diseases such as stenosis or inflammation because exogenous food or digestive fluids pass through them. Stenosis is the most common disorder of the digestive systems. Esophageal stricture is one of the major complications in symptomatic gastroesophageal reflux [1], which is caused by medication-induced stricture (alendronate, phenytoin, and tetracycline), radiation therapy, peptic stricture, and extrinsic compression [2-6]. Benign Biliary stricture (BBS) is an uncommon disease that narrows the common bile duct lumen, which moves the bile from liver to small intestine [7]. The balloon dilation for the bile duct stricture was reported to provide the immediate expansion of the obstructed duct. However, the incidence rate of restenosis after the balloon dilation is still up to 47% [8, 9]. The recent studies presented the development of optical diffusers to circumferentially transmit laser light and to uniformly irradiate tubular tissue structure for thermal treatment [10]. The proposed optical device could be an effective method to deliver laser light in a radial direction particularly to treat the tissue with narrow lumens.

1.2 Thesis contribution

The aim of the current study is to evaluate the feasible application of an optical diffuser integrated with a balloon catheter to treat tubular stricture in a minimally invasive manner. In Chapter 2, an ex vivo test on porcine bile ducts was performed to evaluate the feasibility of the developed device. In Chapter 3, a temperature-monitored optical treatment test was conducted to prevent undesired thermal injury in clinical practice. Finally, Chapter 4 summarizes the work and presents conclusions and future directions.

1.3 Concept of device

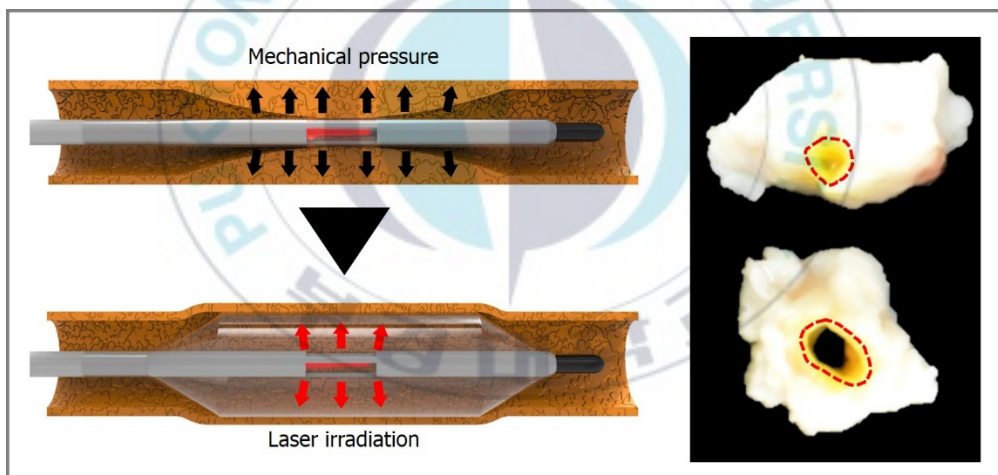


Figure 1. 1. Principle of balloon catheter integrated with optical diffusing applicator

A new biomedical device for treatment of tubular stricture on digestive system was developed by integrating an optical diffusing applicator with a balloon catheter. Mechanical dilation of the balloon secured luminal space in the tubular tissue and centered the optical diffuser. Cylindrical light emission at low irradiance developed

consistent temperature in the lumen. Application of mechanical pressure and optical energy could lead to structural expansion in the biliary duct.



Chapter 2: Integration of optical applicator with balloon catheter for photothermal treatment of biliary stricture

2.1 Abstract

Bile duct stricture is an uncommon disease in gastroenterology resulting from postoperative trauma. In spite of non-surgical treatments, clinical outcomes for the biliary strictures still encounter high restenosis and stent migration. The objective of the current study was to investigate the feasible application of a balloon catheter-integrated diffusing applicator to thermally treat the bile duct stricture. 400- μm optical fibers were micro-machined and then integrated with an inflatable balloon catheter. The fabricated applicator was tested on porcine bile ducts with 20-W 980 nm laser light for 60 s, and a thermal camera was used to measure thermal response of the tissue. Due to mechanical pressure, the inflated balloon was able to expand the tissue lumen up to 6 mm in diameter. Compared to control, the inner area of the treated tissue was increased by four fold (i.e., $2.74 \pm 0.05 \text{ mm}^2$ for treated vs. $0.73 \pm 0.14 \text{ mm}^2$ for control) during the balloon catheter-assisted laser irradiation. The laser-induced tissue temperature reached up to $80.1 \pm 6.4 \text{ }^\circ\text{C}$ (thermal gradient = $1.2 \text{ }^\circ\text{C/s}$). A thin layer of coagulation necrosis ($0.5 \pm 0.1 \text{ mm}$) consistently formed around the lumen. The proposed balloon catheter-integrated diffusing applicator can be a feasible minimally invasive device to photothermally treat the obstructive bile ducts.

2.2 Introduction

Benign Biliary stricture (BBS) is an uncommon disease that narrows the common bile duct lumen, which moves the bile from liver to small intestine [7]. Symptoms include cholangitis, abdominal discomfort, jaundice, and biliary fistula [11]. The etiology of the BBS is associated with postoperative injury after laparoscopic cholecystectomy, pancreatitis, and primary sclerosing cholangitis [12]. Typically, the injury causes an inflammatory response in the tissue, which leads to collagen accumulation, fibrosis, and the eventual obstruction of the bile duct [13]. To define the extent of the stricture, endoscopic retrograde cholangiopancreatography (ERCP) has often been used in clinical situations [14]. During ERCP, two non-surgical treatments can conventionally be performed to reduce the symptoms of the biliary obstruction: balloon dilation and mechanical stenting. The balloon dilation for the bile duct stricture was reported to provide the immediate expansion of the obstructed duct. However, the incidence rate of restenosis after the balloon dilation is still up to 47% [8, 9]. Endoscopic placement of multiple plastic stents or self-expandable metal stents can secure the opening of the bile duct for a long period of time, but the stenting can be associated with stent migration and clogging [15, 16]. Furthermore, the multiple stenting requires multiple ERCP sessions over the one-year period, which results in increase in costs and decrease in patient compliance [17].

The recent studies presented the development of optical diffusers to circumferentially transmit laser light and to uniformly irradiate tubular tissue structure

for thermal treatment [10]. The physical deformation of the fiber surface leads to scatter the transmitted laser light along the fiber, resulting in the cylindrical distribution. In turn, the radial light diffusion from the fabricated fiber entails irreversible tissue denaturation in the tubular tissue structure such as urethra [10]. Due to lower irradiance than the flat-cut fiber (i.e., 13.5 kW/cm^2 for diffuser vs. 64.9 kW/cm^2 for flat fiber), the diffuser reportedly generated up to 50% lower peak temperature and up to 90% thermal gradient in vein [18]. Histological analysis also confirmed that coagulative necrosis was consistently developed around the lumen within 1 mm [10]. The proposed optical device could be an effective method to deliver laser light in a radial direction particularly to treat the tissue with narrow lumens.

The similar concept of photothermal treatment using a laser-catheter system was investigated and clinically applied in 1980s for vascular angioplasty [19]. However, the clinical outcome was unsatisfactory due to stricture, restenosis, or perforation [20]. Unlike the previous fibers, the currently proposed device is associated with reliable fabrication by laser micromachining and consistent radial distribution of high power laser light [10]. On account of advancement of laser technology, laser power and irradiation times can be readily modulated to shorten the preheating time, which was problematic in the previous study, and to regulate the degree of thermal denaturation [21]. In addition, the integration of the proposed device with a temperature sensor can real-time monitor the interstitial tissue temperature during surgical procedures, possibly minimizing complications such as restenosis or perforation that are expected to be less than in the previous studies.

The current study aims to evaluate the feasible application of an optical diffuser integrated with a balloon catheter to treat BBS in a minimally invasive manner. To the best of our knowledge, this study demonstrates the first experimental report to test laser coagulation with the diffusing applicator on bile duct. It was hypothesized that the radial light diffusion could irreversibly denature the mucosal layers in the duct while the balloon dilation could simultaneously provide mechanical expansion to secure the sufficient lumen size. High power infrared laser was used to micro-machine the optical diffuser for circumferential light irradiation, which was then combined with a 20-mm long inflatable balloon prior to tissue testing. A 980-nm laser was employed to coagulate the bile duct *ex vivo* to achieve any structural deformation. A thermal camera was also used to monitor spatio-temporal developments of temperature in the tissue *in situ* during the irradiation. Both gross and histology images were post-experimentally compared between control and treated tissues to identify structural variations and lumen expansion.

2.3 Materials and Methods

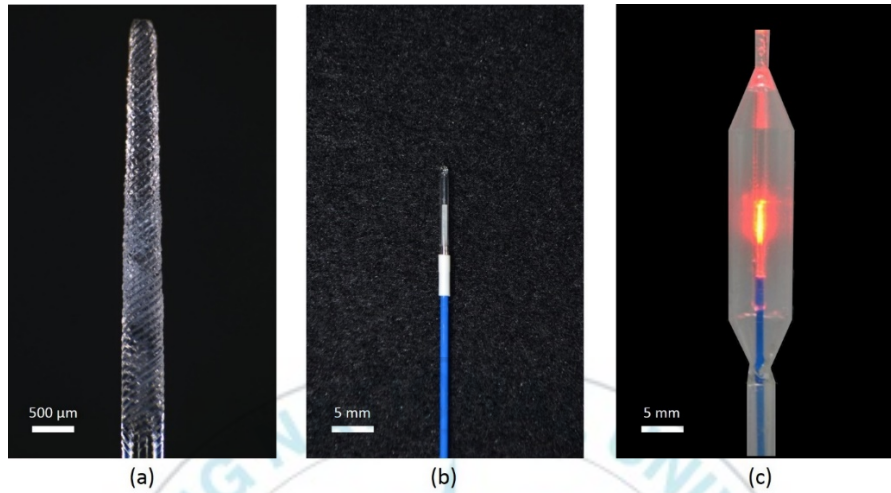


Figure 2. 1. Images of fabricated diffusing applicator for tissue testing: (a) micro-machined surface, (b) glass-capped fiber tip, and (c) balloon catheter-integrated diffuser

To prepare a diffusing applicator, 400- μm multimode optical fibers ($NA = 0.39$, FT400EMT, Thorlabs, Newton, NJ, USA) were used for the current study. A 30-W CO_2 laser (Firestar V30, SYNRAD, WA, USA) in conjunction with motion stages was employed to micro-machine multiple lozenge patterns on the fiber surface for light diffusion and thus, the diffusion length was 5 mm as shown in Figure 2. 1(a). The fabricated diffusing tip was covered with a 27.5-mm long glass cap (outer diameter = 1.5 mm) and sealed with epoxy to prevent any mechanical shock and to firmly position the fiber tip at the center of the glass cap. Then, the proximal end of the glass cap was wrapped by a heat shrinkable tube to maintain a structural integrity during irradiation

on tissue as shown in Figure 2. 1(b). Finally, a 20-*mm* long inflatable polyethylene terephthalate (PET) balloon (Vention Medical, Salem, NH, USA) was added to the distal end of the diffuser to create a balloon catheter-integrated diffusing applicator. Air was supplied through the tube to the catheter at 2 *psi* in order to fully inflate the balloon, and the maximum inflation diameter was 6 *mm*. Figure 2. 1(c) demonstrates an image of the inflated diffusing applicator that spreads HeNe light in a circumferential manner from the middle of the balloon catheter. To identify spatial distribution of light emission, the fabricated diffuser was validated by using a customized goniometer in conjunction with HeNe laser, based upon the previous study [10]. A photodiode sensor with an active area of 1 *cm*² was rotated around the middle point of the diffuser at a radius of 52 *mm* with an increment of 2° (i.e., spatial resolution = 50 μ *m*) to measure polar emissions. In addition, the sensor was translationally moved along the diffuser with an increment of 0.5 *mm* to evaluate longitudinal emissions at various locations of the diffuser. A plastic slit with an area of 1.5 × 1.5 *cm*² was placed between the fiber and the sensor to localize the measured positions during the tests. All the measured light intensities were normalized to minimize the effect of variations of the laser power on the quantitative evaluation.

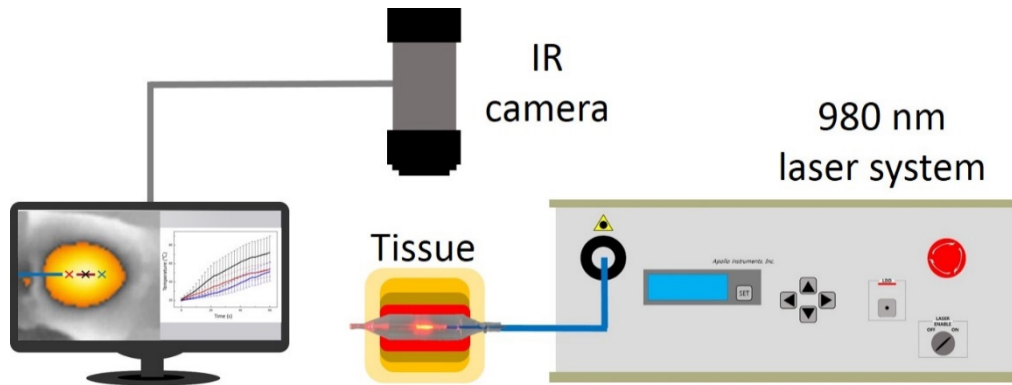


Figure 2. 2. Experimental set-up of balloon catheter-assisted photocoagulation

For *ex vivo* tissue testing, porcine bile ducts were procured from Inha University Hospital in Incheon, Korea and used as sample specimens. The samples were stored at 4°C to prevent any dehydration and structural deformation prior to the testing. The tissue was 3-*cm* long with an inner diameter of 1.05 *mm* and a wall thickness of 0.68±0.26 *mm*. Figure 2. 2 demonstrates an experimental set-up for photocoagulation with a balloon catheter-integrated diffusing applicator. A continuous-wave near IR wavelength ($\lambda = 980 \text{ nm}$, Apollo Instruments, Irvine, CA, USA) was implemented as a light source to entail irreversible thermal denaturation in the tissue. The applied power was set at 20 *W* and the irradiation times varied from 0 to 60 *s* during the tests. Initially, the diffuser tip was placed in the bile duct and was completely made contact with the inner wall of the tissue. Then, the balloon was fully dilated to expand the duct prior to the laser irradiation. A thermal IR camera (A325sc, FLIR, Inc., Oregon, USA) was positioned 40 *cm* above the tissue specimen and implemented to monitor temperature variations on the tissue surface during the irradiation ($N = 3$). The recorded data was

transferred to a computer, and both thermal images and temperature information were post-experimentally analyzed. For histological analysis, both control and treated tissue samples (20 W for 60 sec) were stored at neutral formalin and dehydrated with gradient ethanol series. After dehydration, the tissues were embedded in paraffin and sectioned at 4 mm onto slide. The samples were rehydrated and stained by using hematoxylin and eosin (H&E). Harris hematoxylin and eosin U were purchased from Sigma (St. Louis, MO, USA) and BBC Biochemical (Mount Vernon, WA, USA), respectively. Xylene, ethanol, and formalin were purchased from Daejung Inc. (Daejeon, Korea). Permount® was purchased from Fisher (Waltham, MA, USA). Microscopic images were then obtained using a light microscope (Olympus BX51, Hamburg, Germany) at the magnification of 40. Image J (National Institute of the Health, Bethesda, MD, USA) was used to estimate the physical dimensions of the lumen size and the degree of tissue coagulation ($N = 5$). For non-parametric statistical analysis, Mann-Whitney U test was performed and $p < 0.05$ represents significant.

2.4 Results

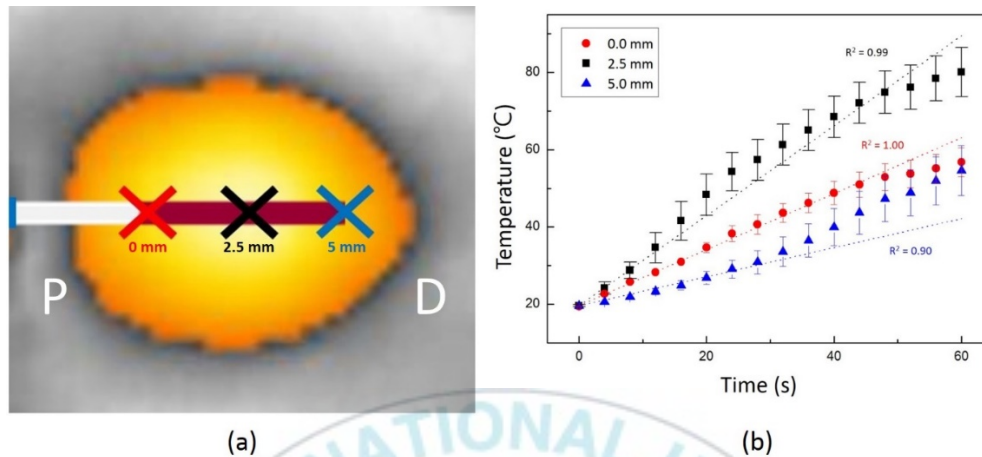


Figure 2. 3. Thermal imaging on *ex vivo* porcine tissue during photocoagulation at 20 W: (a) IR image captured at 60 s after irradiation and (b) temporal development of temperature at various points of 0, 2.5, and 5 mm from proximal end of diffusing tip (P = proximal and D = distal ends; $N = 3$)

Figure 2. 3(a) displays a thermal image of porcine tissue captured at 60 s after irradiation at 20 W with a diffusing applicator. Due to light diffusion, the spatial distribution of temperature (yellow) showed an elliptical shape. Based upon the acquired thermal imagers, the degree of temperature elevation was evaluated at three fixed points (i.e., red, black, and blue points), where were 0, 2.5, and 5 mm from the proximal end of the diffuser tip. Figure 2. 3(b) exhibits temperature variations at the three points as a function of irradiation time. Compared to the two points (0 and 5 mm), the middle point (2.5 mm) presented 40% higher temperature increase. After 60-s irradiation, the temperature at the middle point reached 80.1 ± 6.4 °C at the thermal gradient of 1.2 °C/s. Both the proximal (0 mm) and the distal (5 mm) ends demonstrated

almost comparable developments of the tissue temperature up to 56.8 ± 3.8 (i.e., $0.7 \text{ }^\circ\text{C/s}$) and $54.6 \pm 6.4 \text{ }^\circ\text{C}$ (i.e., $0.4 \text{ }^\circ\text{C/s}$), respectively. It was noted that after 60-s photocoagulation, the tissue temperature was close to the temperature for irreversible thermal denaturation (i.e., $65\sim 75 \text{ }^\circ\text{C}$ [22]).

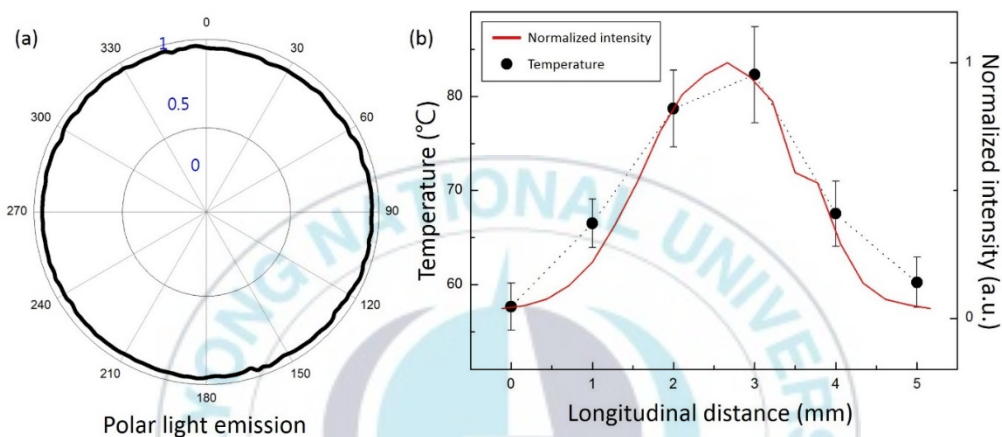


Figure 2. 4. Spatial light distribution of diffusing applicator: (a) polar light emission (0.96 ± 0.02) and (b) temperature measured 60 s after laser irradiation and normalized longitudinal intensity at various fiber points (0 mm = proximal end and 5 mm = distal end; $N = 3$)

Figure 2. 4 demonstrates spatial light distribution from a diffuser applicator measured by a goniometer. Figure 2. 4(a) displays polar emissions measured at the center of the diffuser tip (i.e., 2.5 mm). Apparently, the diffuser yielded almost isotropic light distribution in all directions as the normalized intensities were measured to be 0.96 ± 0.02 . Figure 2. 4(b) displays temperature measured at 60 s after laser irradiation (left axis) and normalized longitudinal intensity (right axis) as a function of longitudinal distance from the proximal end of the diffuser ($N = 3$). Overall, the temperature profile

(black dotted line) showed a good agreement with the distribution of optical energy (red solid line) along the diffuser. The maximum temperature of 82.3 ± 5.1 °C occurred at 3 mm, where the peak intensity was emitted as shown in Figure 2. 4(b). Both the temperature and the intensity distributions almost mirrored a Gaussian profile due to the current micromachining method for the diffuser.

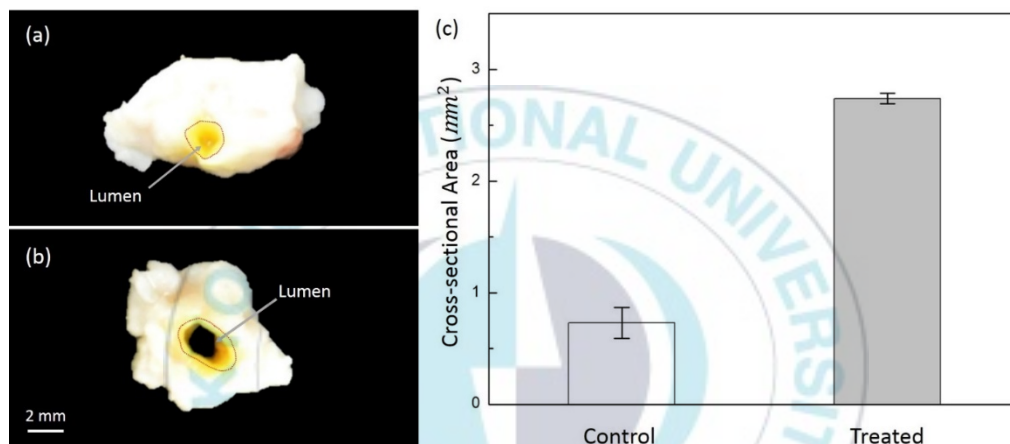


Figure 2. 5. Comparison of porcine bile ducts: (a) control, (b) treated tissue and (c) quantitative comparison of cross-sectional area variations between pre- and post-treatments ($N = 5$)

Figure 2. 5 compares porcine bile ducts pre- and post-treatment with a balloon-assisted diffusing applicator. Figure 2. 5(a) shows a control tissue containing a lumen with an inner diameter of 1.2 mm. After photocoagulation at 20 W for 60 s, the inner diameter of the lumen increase up to 2.2 mm, which was 83% larger than the control case. The degree of thermal coagulation was measured to be 204 ± 29 μm as shown in Figure 2. 5(b). The cross-sectional areas of the lumens were quantitatively compared

between the control and the treated tissue in Figure 2. 5(c). Apparently, the treat tissue created the lumen area of $2.74\pm 0.05 \text{ mm}^2$, which was almost four-fold enhancement, compared to the control (i.e., $0.73\pm 0.14 \text{ mm}^2$; $p < 0.001$). To assess the photocoagulation effect of laser on the bile duct, histological analysis was performed on the control and the treated tissue in Figure 2. 6. As shown in Figure 2. 6(a), a normal bile duct consists of lumen, mucosa, submucosa, and adventitia, of which the entire thickness was measured to be $0.6\pm 0.3 \text{ mm}$. The submucosa exhibited a complex of smooth muscle and connective tissues whereas the adventitia represented an outer boundary of the duct. After irradiation at 20 W for 60 s, coagulation necrosis ($0.5\pm 0.1 \text{ mm}$) took place at the lesion from the mucosa to the adventitia. The villi of mucosa were collapsed and only connective tissue remained as shown in Figure 2. 6(b). It should be noted that the diffuser-assisted photocoagulation entailed circumferential thermal denaturation with almost uniform coagulation thickness in a radial direction.

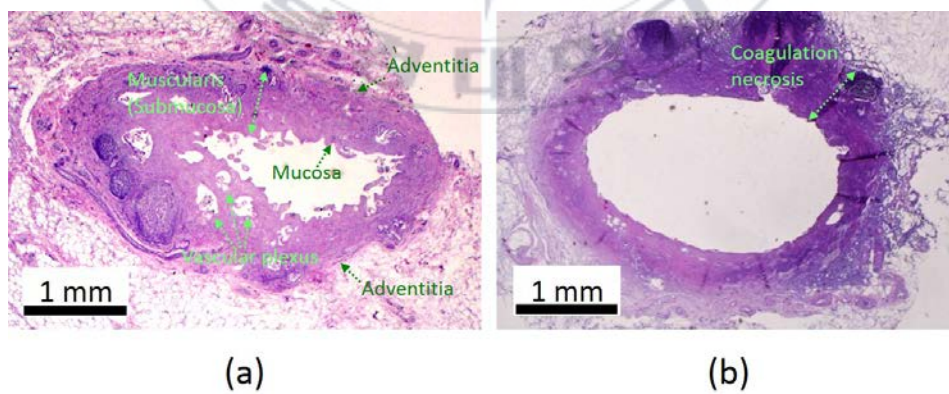


Figure 2. 6. Histological comparison ($\times 40$) after 20-W photocoagulation for 60 s: (a) control and (b) treated tissue stained by H&E

2.5 Discussion

The goal of the current study was to demonstrate the feasibility of a balloon-assisted diffusing applicator for achieving thermo-mechanical deformation of biliary tissue structure. Regardless of measurement points, linear variations in temperature ($R^2 = 0.90 \sim 1.00$) implicated that irreversible tissue responses could be predictable due to thermal dependence (Figure 2. 3). On the other hand, comparable temperature elevations were found at the proximal and distal ends whereas the maximum temperature occurred at the center of the tip. It is conceived that the observed thermal gradients resulted from non-uniform distribution from longitudinal emissions (Figure 2. 4(b)), which may similarly affect spatial profile of thermal denaturation in the tissue. However, in spite of the position-dependent temperature developments, considerable variations in tissue coagulation were hardly distinguished in the current study possibly due to a short range of laser treatment on the tissue ($\leq 7 \text{ mm}$) and conductive heat transfer. Moreover, goniometric measurements confirmed that polar emissions were quite circular (0.96 ± 0.02) along the entire diffusing tip (Figure 2. 4(a)), essentially obtaining the circumferential distribution of the irreversible thermal coagulation (Figure 2. 6(b)). Further investigations are currently underway to incorporate various etching methods with micromachining technique in order to develop more uniform and homogeneous longitudinal light emissions. The desirable overall emission distribution would be a cylindrical profile with less optical/thermal gradients to eventually achieve consistent tissue deformation along the diffusing applicator.

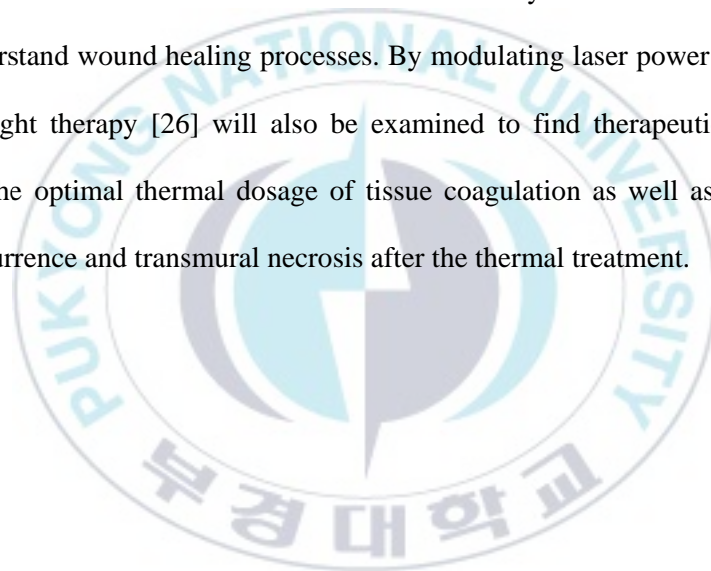
The current study selected PET material for a noncompliant dilation balloon due to high burst pressures (up to 400 *psi*), optical clearance, and high melting point (260 °C). The preliminary study confirmed that the transmission loss of the PET layer was approximately 13% during 20-W 980 *nm* irradiation. In spite of slight light absorption, no significant physical deformation of the balloon (melting or partial damage) was observed after thermal treatment of tubular tissue. However, the wall thickness of the balloon is typically less than 100 μm , implying that the thin balloon may still be vulnerable to sudden temperature elevation and higher power irradiation. In fact, previous studies demonstrated that the balloon behaved as a thermal insulating barrier due to different thermal conductivities between PET and air inside the balloon [23, 24]. The insulation effect helped rapidly develop the interstitial temperature up to 100 °C. A wide range of wavelengths and optical power will thus be examined to identify the optimal balloon materials for safe photothermal treatment by monitoring material-dependent temperature variations. Additionally, unlike standard balloons used in the current study, various shapes of the balloons (e.g., conical/square balloon) need to be evaluated to develop a simple fabrication method to integrate a diffusing applicator with the balloon.

Bile duct is a multi-layered tissue consisting of mucosa, submucosa, and adventitia (Figure 2. 6(a)). According to Figure 2. 6(b), the propose applicator entailed the irreversible thermal coagulation up to 0.5 *mm*, covering more than 80% of a cross-sectional area of the biliary tissue. During laser treatment, fibrosis often results from

severe thermal injury. Since the bile duct is primarily a passage to carry bile for food digestion, the villi of the mucosa needs to regrow or be partially preserved to recover the biliary function even after the thermal treatment. In addition, our preliminary study presented that once even thin thermal coagulation layers were consistently developed in the peripheral rim of the tubular tissue, the lumen could maintain the structurally deformed shape. Accordingly, the extent of the thermal denaturation should be identified and optimized simultaneously to achieve the luminal expansion, to preserve the biliary function, and to minimize re-fibrosis. A number of laser parameters such as wavelength, pulse mode, optical power, and irradiation time should also be tested by using response surface methodology for systematic evaluations [25]. Recently, inhibition of fibroblast-myofibroblast transition was investigated with low intensity diode laser irradiation in terms of expression of collagen-related genes and tissue inhibitor [26]. Thus, application of dual-wavelengths will be performed to limit fibrotic responses and even to reverse the fibrotic patterns after the photothermal treatment on the biliary ducts.

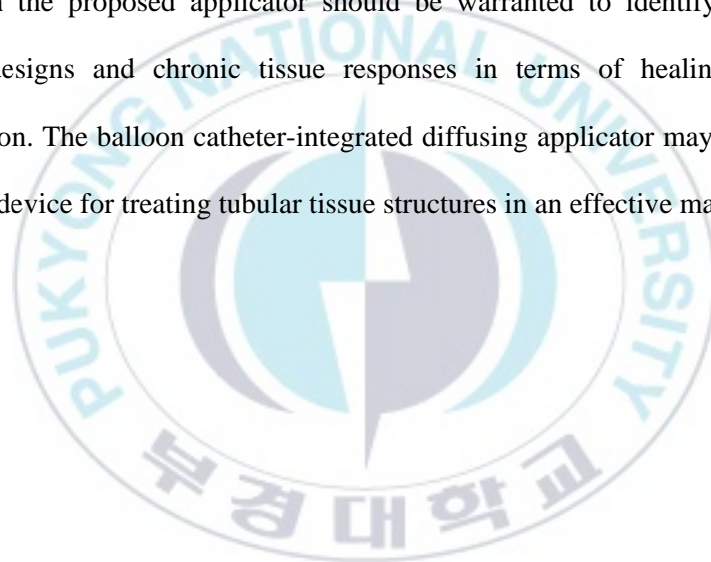
A balloon catheter-integrated diffusing applicator was able to vividly secure luminal expansion with an 83% area increase (Figure 2. 5) after photothermal treatment. The structure integrity was circumferentially maintained in a circular shape on account of formation of thermal coagulation layers in tissue (Figure 2. 6). However, as normal biliary tissue was tested for the entire testing, biliary stricture with narrowed channels may accompany diverse physical responses to laser treatment in terms of thermal

denaturation and mechanical deformation. No *in vivo* tests has been conducted yet in order to validate the clinical feasibility of the proposed applicator. Thus, porcine animal models with biliary stricture are currently under development by using a radiofrequency (RF) device to induce severe thermal injury to bile ducts for fibrosis. The *in vivo* testing will explore the optimal range of balloon dilation and mechanical pressure to achieve permanent structural deformation. The photothermal interactions with the *in vivo* diseased tissue will be evaluated to identify acute and chronic responses and to understand wound healing processes. By modulating laser power and applying low laser light therapy [26] will also be examined to find therapeutic methods to determine the optimal thermal dosage of tissue coagulation as well as to minimize fibrosis recurrence and transmural necrosis after the thermal treatment.



2.6 Conclusion

A balloon catheter-integrated diffusing applicator was evaluated ex vivo for photothermally treating biliary tissue structure. Both mechanical dilation and light diffusion were contributed to expand the lumen of the bile duct accompanying uniform coagulative necrosis. Lower irradiance along the diffuser was able to circumscribe the temperature increase near the threshold of irreversible thermal denaturation. In vivo testing with the proposed applicator should be warranted to identify the optimal treatment designs and chronic tissue responses in terms of healing and tissue reconstruction. The balloon catheter-integrated diffusing applicator may be a feasible therapeutic device for treating tubular tissue structures in an effective manner.



Chapter 3: Temperature-monitored optical treatment for radial tissue expansion

3.1 Abstract

Esophageal stricture occurs in 7~23 % of patients with gastroesophageal reflux disease. However, the current treatments including stent therapy, balloon dilation, and bougienage involve limitations such as stent migration, formation of the new strictures, and snowplow effect. The purpose of the current study was to investigate the feasibility of structural expansion in tubular tissue *ex vivo* during temperature-monitored photothermal treatment with a diffusing applicator for esophageal stricture. Porcine liver was used as an *ex vivo* tissue sample for the current study. A glass tube was used to maintain a constant distance between the diffuser and tissue surface and to evaluate any variations in the luminal area after 10-W 1470-nm laser irradiation for potential stricture treatment. The 3D goniometer measurements confirmed roughly isotropic distribution with less than 10 % deviation from the average angular intensity over 2π (i.e., 0.86 ± 0.09 in arbitrary unit) from the diffusing applicator. The 30-s irradiation increased the tissue temperature up to 72.5 °C, but due to temperature feedback, the interstitial tissue temperature became saturated at 70 °C (i.e., steady-state error = ± 0.4 °C). The irradiation times longer than 5 s presented area expansion index of 1.00 ± 0.04 , signifying that irreversible tissue denaturation permanently deformed the lumen in a circular shape and secured the equivalent luminal area to that of the glass tube.

Application of a temperature feedback controller for photothermal treatment with the diffusing applicator can regulate the degree of thermal denaturation to feasibly treat esophageal stricture in a tubular tissue.



3.2 Introduction

Esophageal stricture is one of the major complications in symptomatic gastroesophageal reflux [1], which is caused by medication-induced stricture (alendronate, phenytoin, and tetracycline), radiation therapy, peptic stricture, and extrinsic compression [2-6]. Esophageal stricture occurs in 7 - 23 % of untreated patients with gastroesophageal reflux disease (GERD) [27]. GERD is the most common cause of benign esophageal stricture and affects roughly 40 % of adults in united states populations [28, 29]. Common treatments for the esophageal stricture include fluoroscopic placement of expandable esophageal stents, balloon dilation, and bougienage due to high efficacy to widen a passageway [30-33]. However, the incidence rate of chronic complications often ranges from 40 to 100 % in association with stent migration and formation of the new strictures [30]. As the size of bougies must be larger than the area of stricture, the bougienage can result in a snowplow effect that leads to undesirable local tissue injury [34]. Moreover, the stent therapy for the esophageal disease is often associated with high cost (\$ 1,000~2,000 per stent) and difficult stent removal a few months after the deployment [35].

To reduce complication rates, interstitial laser therapy has been implemented as a minimally invasive treatment. Laser ablative/coagulative treatment is an in situ technique for treating benign or malignant tumors in various organs such as liver, stomach, and brain [36, 37]. Volumetric heating within the target tissues during laser irradiation leads to immediate tissue necrosis and eventual tumor death [38]. However,

the laser light is typically transmitted through an end-firing or side-firing optical fiber. Thus, optical energy is delivered merely in one direction, limiting the range of the laser treatment [10]. In order to overcome this limitation, diverse fiber tips have been designed and developed [39]. In particular, a cylindrically diffusing optical applicator were designed and evaluated to treat tubular tissue structures such as trachea, bile duct, blood vessel, and urethra [10]. The recent studies presented the development of the optical diffusers to circumferentially transmit laser light and to uniformly irradiate tubular structures for thermal treatment [10]. The physical deformation of the fiber surface leads to scatter the transmitted laser light along the fiber, resulting in the cylindrical distribution. In turn, the radial light diffusion from the fabricated fiber entails irreversible tissue denaturation in a circumferential manner [10].

The purpose of the current study was to investigate the feasibility of structural expansion in tubular tissue *ex vivo* during temperature feedback-assisted photothermal treatment. It was hypothesized that both circumferential light emission and constant temperature application could entail irreversible tissue deformation in a radial direction and eventually secure a cylindrical channel within the tissue. A temperature controller with a thermocouple was applied to monitor the interstitial tissue temperature real-time during the irradiation. An optical diffusing applicator was employed to deliver a 1470-*nm* wavelength to initiate photothermal interactions in the tissue. The extent of thermal coagulation as well as area variations were quantitatively compared at various irradiation times.

3.3 Method and Materials

Porcine liver was used as an *ex vivo* tissue sample for the current study and was harvested from a local slaughter house. Initially, the tissue was frozen at $-15\text{ }^{\circ}\text{C}$ for an hour to cut specimens in size of $2 \times 2\text{ cm}^2$, and a small hole in 5-mm diameter was created in each sample in order to insert a glass tube (outer diameter = 5 mm , length = 6 cm). The glass tube was used to secure a cylindrical channel inside the tissue and to evaluate any variations in the luminal area after laser irradiation for potential stricture treatment. A customized optical diffusing applicator ($400\text{-}\mu\text{m}$ core-diameter and 5-mm diffusing tip; TeCure, Busan, Korea) was employed to achieve circumferential light distribution. To characterize spatial distribution of the light emission, the diffuser was validated by using a customized goniometer, based upon the previous study [10]. A photodiode sensor (PD-300-3W, Ophir, Jerusalem, Israel) with an active area of 1 mm^2 was rotated around the proximal end of the diffuser at a radius of 2 mm with an increment of 2° (i.e., spatial resolution = $50\text{ }\mu\text{m}$) to measure polar emissions. After the measurements, the diffuser was translated along the diffuser axis by 0.5 mm toward the distal end, and the same polar measurement was performed for the entire diffusing tip (5 mm) in order to reconstruct 3D polar emission profiles. Due to the limited spectral range of the photodiode ($350\text{--}1100\text{ nm}$), HeNe laser was used to visualize the light emission from the diffusing tip. All the measured light intensities were normalized by the maximum intensity measured from the middle position of the diffuser to minimize the effect of variations in the laser power on the quantitative evaluation.

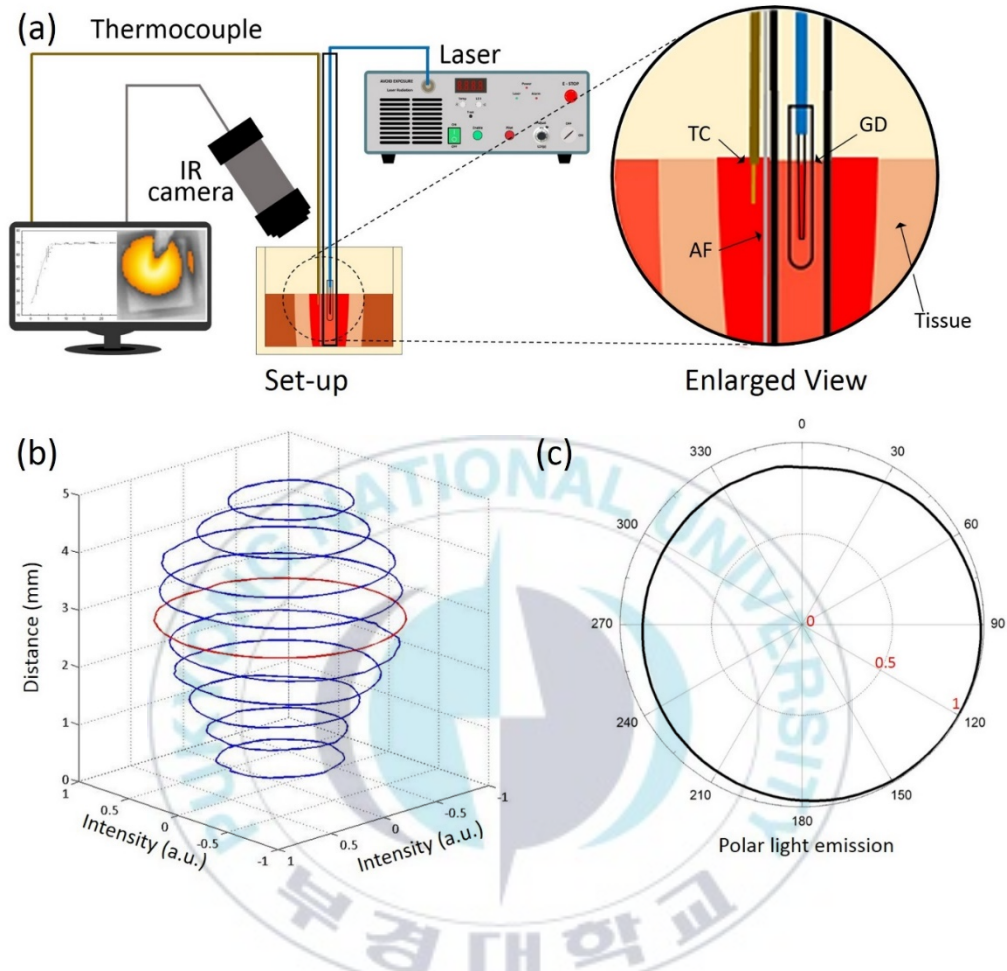


Figure 3. 1. (a) Experimental set-up for *ex vivo* laser photocoagulation assisted with temperature monitoring and normalized spatial light distribution based on goniometer measurements: (b) 3D emission profile along diffuser and (c) polar light emissions from middle

Figure 3. 1(a) demonstrates an experimental set-up for *ex vivo* laser photocoagulation assisted with temperature monitoring. A laser system ($\lambda = 1470 \text{ nm}$, Changchun New Industries Optoelectronics Tech, Changchun, Jilin, China) was implemented as a light source to entail irreversible thermal denaturation in tissue. The initial applied power was set at 10 W and various irradiation times (5, 10, 20, 30, 60,

and 120 s; $N = 5$) were applied during the tests. The average irradiance on the tissue surface was estimated to be around 21.6 W/cm^2 . To emulate mechanical inflation in a tubular tissue structure, a glass tube was inserted into the pre-created hole in the tissue specimen and secured a channel for diffuser insertion. A K-type thermocouple (TSL-101, Guageworld, Anyang, Korea) was also attached to the outer surface of the glass tube in an attempt to real-time monitor the interstitial tissue temperature (accuracy of $\pm 1.2 \text{ }^\circ\text{C}$) during irradiation. To prevent any self-heating from direct light absorption by the thermocouple, 1-mm wide aluminum foil was placed between the glass tube surface and the thermocouple. Preliminary tests confirmed no temperature increase due to the heating at the foil. During the tests, the thermocouple was in full contact with the tissue surface, and temporal development of temperature was recorded at 25 Hz by a DAQ module (OMB-DAQ-55, OMEGA Engineering, Inc., CA, USA). A temperature controller (TK4M-14CN, Autonics Europe, Wehl, Netherlands) was used to maintain the constant interstitial tissue temperature at $70 \text{ }^\circ\text{C}$ during the irradiation, which is close to the temperature for irreversible tissue denaturation (i.e., $65\text{--}75 \text{ }^\circ\text{C}$) [22]. Then, the prepared diffusing applicator was placed at the center of the glass tube. A thermal IR camera (A325sc, FLIR, Inc., Oregon, USA) was positioned 40 cm above the tissue specimen and implemented to monitor temperature variations on the tissue surface during the laser application. The recorded temperature data were transferred to a computer and temperature information were post-experimentally analyzed. A digital camera (D5100, Nikon, JPN) was implemented to photograph any luminal deformation in the tissue. Image J (National Institute of the Health, Bethesda, MD, USA) was used

to quantify physical dimensions of coagulation thickness as well as luminal area in the treated tissue specimens. For histological analysis, each tissue sample was stored at neutral formalin for five days and dehydrated with gradient ethanol series. After the dehydration, the tissues were embedded in paraffin. The samples were rehydrated and stained by using hematoxylin and eosin (H&E). Harris hematoxylin and eosin U were purchased from Sigma (St. Louis, MO, USA) and BBC Biochemical (Mount Vernon, WA, USA), respectively. Xylene, ethanol, and formalin were purchased from Daejung Inc. (Daejeon, Korea). Microscopic images were then obtained by using a light microscope (Olympus BX51, Hamburg, Germany) and CellScan (Olympus, Miami, FL, USA) at the magnification of 125. For statistical analysis, Mann-Whitney U test as non-parametric analysis using SPSS was performed and $p < 0.05$ represents insignificance. Figure 3. 1(b) and 3. 1(c) demonstrate spatial light distribution of a diffusing applicator estimated from goniometric measurements. Figure 3. 1(b) displays a 3D emission profile along the axis of the diffusing applicator. The light intensity was normalized by the maximum intensity measured from the middle position of the diffuser (red color). A series of concentric circles indicated that the light was distributed circumferentially around the diffuser regardless of axial distance. The normalized intensity was slightly skewed to the distal end of the diffuser (i.e., 5 mm). Figure 3. 1(c) shows a polar emission profile from the middle position of the diffusing applicator (i.e., 2.5 mm away from distal end). The polar results demonstrated roughly isotropic distribution with less than 10% deviation from the normalized angular intensity over 2π (i.e., 0.86 ± 0.09 in

arbitrary unit; Figure 3. 1(b)), indicating homogeneous and circumferential radiation from the diffusing tip.



3.4 Results

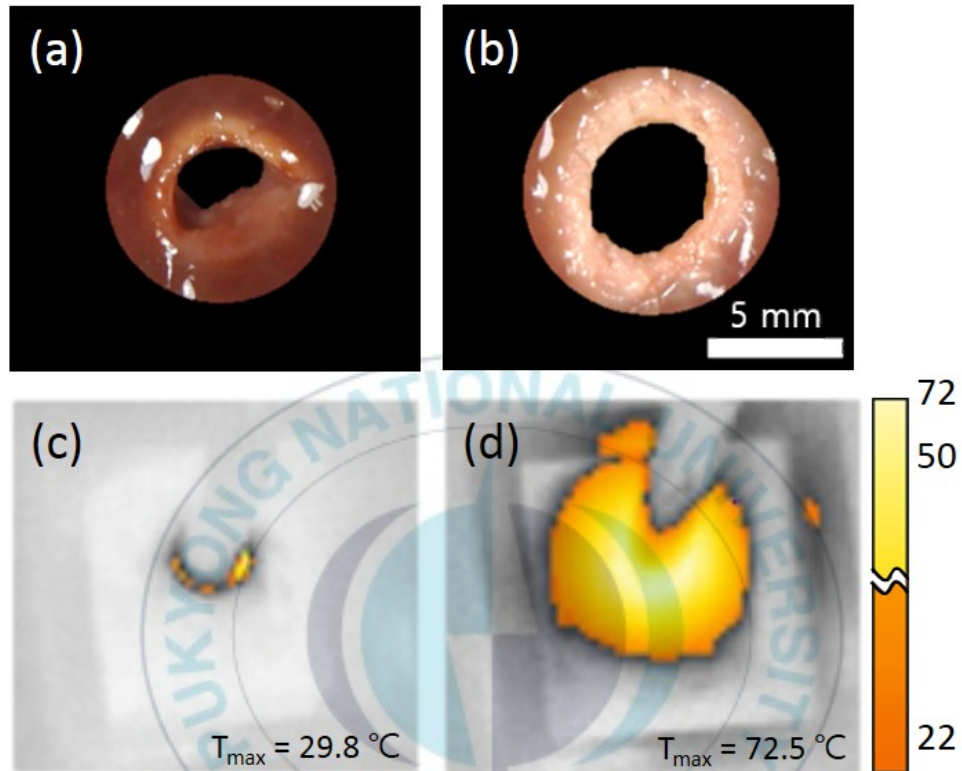


Figure 3. 2. Top-view images of tissues treated for (a) 5 s and (b) 30 s and corresponding thermal IR images acquired at (c) 5 s and (d) 30 s irradiation

Figure 3. 2 presents top-view and corresponding thermal IR images of liver tissue after laser application for 5 s (Figures 3. 2(a) and 3. 2(c)) and 30 s (Figures 3. 2(b) and 3. 2(d)) at 10 W. According to Figure 3. 2(a), the extent of tissue coagulation from the 5-s irradiation was quite superficial (coagulation thickness = $0.6\pm 0.2\text{ mm}$) due to relatively short delivery time of optical energy. The area of the lumen was measured to be $6.3\pm 2.7\text{ mm}^2$, which was 68 % smaller than the initial area of the glass tube (19.6

mm^2) inserted into the tissue. The area reduction indicated that the lumen was collapsed inward due to structural flexibility of the liver after the 5-s irradiation. On the other hand, as the irradiation time increased up to 30 s, the coagulation depth was extended up to 1.3 ± 0.1 mm, which was almost 2-fold thicker than that from the 5-s irradiation ($p < 0.001$; Figure 3. 2(b)). It was noted that irreversible tissue denaturation (discolored area) was vividly developed in a radial direction due to circumferential emissions from a diffusing applicator. In addition, the area of the lumen (18.4 ± 0.7 mm^2) after the 30-s irradiation showed a 3-fold enlargement ($p < 0.001$), compared to that after the 5-s irradiation. As the area of the lumen in a circular shape was close to the area of the inserted glass tube (merely 6% reduction), the thermal coagulation was able to entail the permanent structural deformation in the tissue after the laser application. The IR image captured 5-s after the irradiation in Figure 3. 3(c) showed the maximum temperature of 29.8 °C. However, the 30-s irradiation increased the tissue temperature up to 72.5 °C in Figure 3. 2(d), which is close to the temperature for irreversible thermal denaturation (i.e., 65~75 °C [22]).

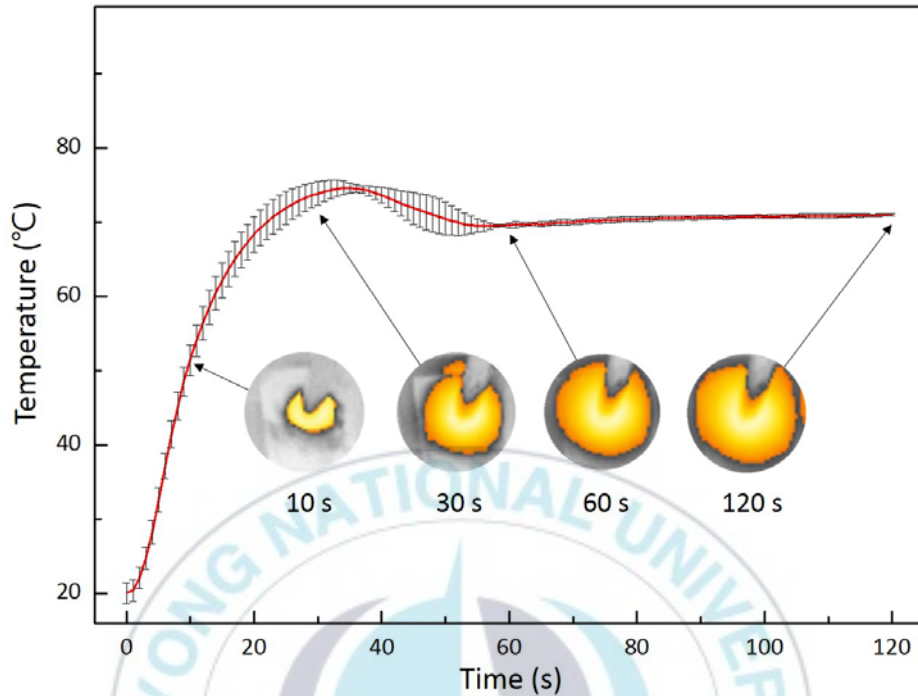


Figure 3. 3. Temporal development of temperature as function of irradiation time measured by thermocouple ($N=5$) and synchronized IR image by thermal camera

Figure 3. 3 displays temporal developments of the interstitial tissue temperature measured by a thermocouple during laser irradiation and the corresponding IR images captured at 10, 30, 60, and 120 s. At 34 s after the irradiation, the tissue reached the maximum temperature of 74.6 °C (transient temperature change = 1.6 ± 0.1 °C/s), and then, the temperature commenced to decrease. Due to feedback from the temperature controller, the temperature became saturated at 70 °C after 58-s irradiation (i.e. steady-state error = ± 0.4 °C). A series of the IR images also confirmed that the extent of the surface temperature increased rapidly with the irradiation time but eventually became almost invariant.

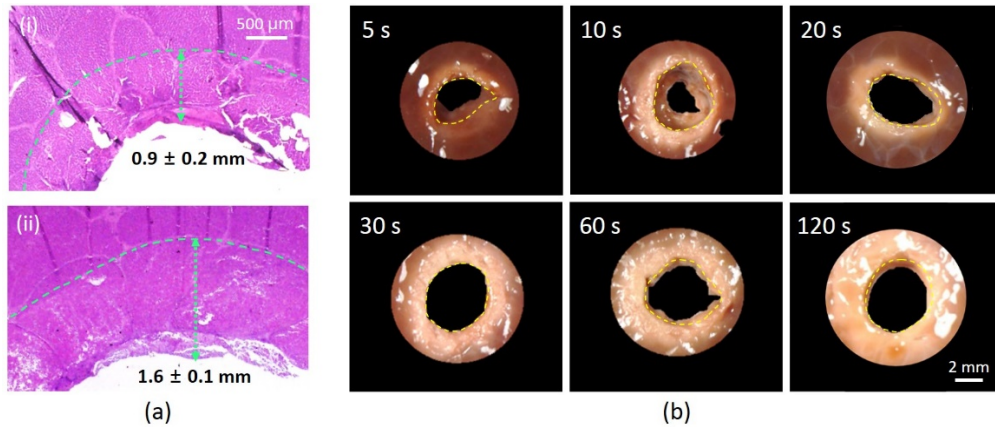


Figure 3. 4. (a) Histology images after 10-W photocoagulation for (i) 10 s and (ii) 60 s ($\times 125$) and (b) luminal deformation in tissue after 10-W photocoagulation for various irradiation times (5, 10, 20, 30, 60, and 120 s)

Figure 3. 4(a) demonstrates histology images of liver tissue after 10-W photocoagulation for 10-s and 60-s irradiation. Due to temperature development and accumulation, both the conditions entailed irreversible thermal denaturation in the tissue. Six-fold longer irradiation time resulted in 80% thicker coagulation depth (i.e., 0.9 ± 0.2 mm for 10 s vs. 1.6 ± 0.1 mm for 60 s; $p < 0.001$). Furthermore, Figure 3. 4(b) represents top-view images of the tissue after photocoagulation at various irradiation times (5, 10, 20, 30, 60, and 120 s). Overall, the extent of irreversible tissue denaturation was augmented gradually by increasing the irradiation times. In the case of the 5-s photocoagulation, partial tissue denaturation occurred as evidenced by tanned discoloration on the surface (12 o'clock). After the glass tube was removed, the surrounding tissue collapsed and partially covered the hole created for the tube insertion. However, once the irradiation time increased to 10 s, circumferential tissue coagulation

ostensibly formed around the hole, and the luminal area became $17.6 \pm 1.0 \text{ mm}^2$, which was almost close to the area of the glass tube (19.6 mm^2). However, partial tissue collapse was still noticed at the bottom of the tissue (Figure 3. 4(b)). The longer irradiation times than 10 s presented almost no variations in the luminal area after the removal of the glass tube, but the coagulation depth continued to increase (i.e., thicker discoloration). It was noted that upon development of the radial coagulation rim on the tissue, the lumen was vividly secured and the luminal area of the tissue was almost invariant. The shape of the lumen was nearly circular, which reflected the geometry of the glass tube inserted into the tissue.

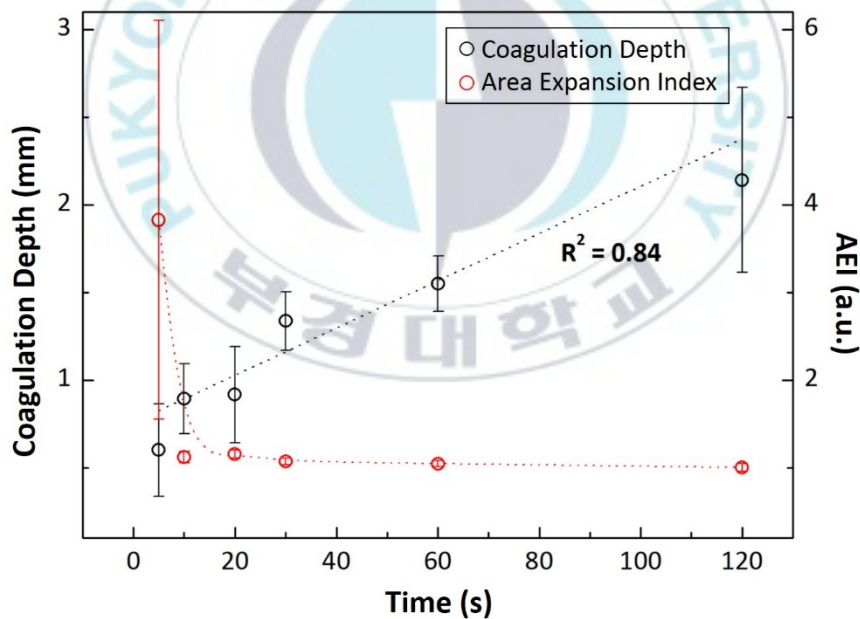


Figure 3. 5. Variations in coagulation depth (black circle; left axis) and area expansion index (AEI, red circle; right axis) as function of irradiation time ($N = 5$; C.D. = coagulation depth, A_i = initial lumen area, and A_f = final lumen area)

Figure 3. 5 displays variations in coagulation depth and area expansion index (AEI) as a function of irradiation time. The index was defined as the ratio of the initial tube area (19.6 mm^2) to the laser-induced area in the lumen in order to evaluate the degree of the luminal dilation after photocoagulation. The coagulation depth increased gradually with the irradiation times and reached $2.1 \pm 0.5 \text{ mm}$ at 120 s. Similar to Figure 3. 4, the shortest irradiation time (i.e., 5 s) involved relatively superficial tissue denaturation ($0.6 \pm 0.2 \text{ mm}$). It was noted that the 120-s irradiation yielded larger standard deviations in the coagulation depth as the tissue surface experienced partial carbonization. In the case of the luminal deformation, the 5-s irradiation was associated with large variations in AEI, in that the surrounding tissue collapsed and haphazardly covered the pre-created hole in the tissue immediately after removal of the glass tube. However, the rest of the irradiation times longer than 5 s presented AEI of 1.00 ± 0.04 , signifying that irreversible tissue denaturation permanently deformed the lumen structure in a circular shape and maintained the equivalent luminal area to that of the glass tube.

3.5 Discussion

The proposed diffuser demonstrated good polar isotropy of irradiation (i.e., normalized intensity of 0.86 ± 0.09) and tissue denaturation (Figures 3. 1 and 3. 4), which was similar to the findings in a previous study [40]. However, due to discontinuities at the proximal end of the diffusing tip, the longitudinal distribution was slightly skewed to the distal end (Figure 3. 1(b)), resulting in asymmetric coagulation in the tissue. In spite of being more homogeneous than commercial cylindrical diffusers [40], the overall longitudinal profile still seemed conical rather than cylindrical (Figure 3. 1(b)). The conical irradiation could adversely cause inhomogeneous tissue denaturation and, thus, less predictable clinical outcomes during photothermal treatment on esophageal stricture. In order to achieve more homogenous longitudinal emissions, an additional melting process on the proximal end of the diffusing tip is currently under investigation. In addition, extra micromachining on the glass cap will be performed to more evenly distribute the diffusing light. Therefore, more cylindrically homogenous light from the diffusing applicator is expected to attain more predictable tissue responses and to control the degree of fibrotic tissue deformation during the photothermal treatment.

The current study exhibited the feasibility of a temperature feedback controller during diffuser-assisted treatment to maintain the equivalent interstitial temperature ($\sim 70\text{ }^{\circ}\text{C}$). Given the testing conditions, the identical tissue temperature led to an almost linear relationship between the extent of coagulation and irradiation time (Figures 3. 4

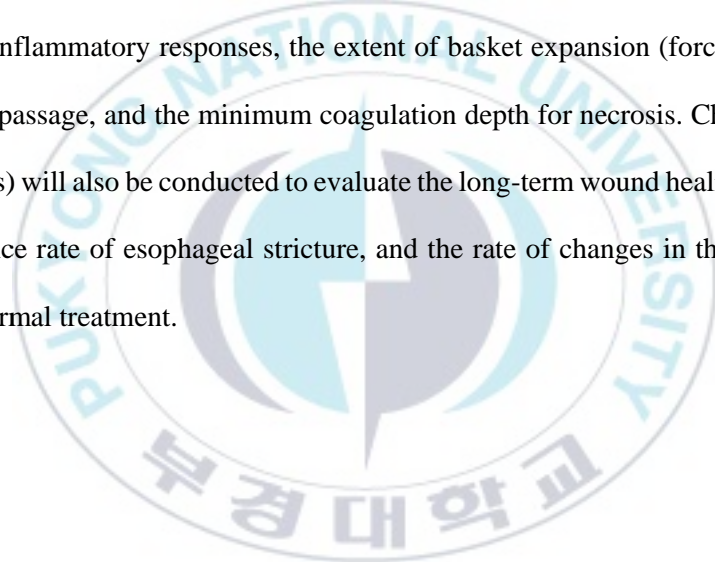
and 3. 5), which well agrees with the findings in a previous study [10]. Thus, it is conceived that simple regulation of the irradiation time may determine the degree of thermal treatment and minimize thermal injury. However, the thermocouple was positioned at the middle of the diffusing tip during the study, which hardly monitored the overall temperature increase. Multiple measurements with the thermocouples at various positions of the tip and the tissue will thus be necessary to predict spatio-temporal distribution of the temperature more precisely and eventually to help maximize clinical outcomes. In addition, the multiple thermocouple measurements can verify the degree of homogeneity for diffusing emission profiles. Furthermore, although 1-*mm* wide aluminum foil was applied on the glass cap surface to prevent self-heating of the thermocouple (Figure 3. 1(a)), the current set-up would be less practical for clinical conditions. Another fiber optic sensor (e.g., fiber bragg grating, FBG) is currently being tested to real-time monitor the interstitial temperature due to no electromagnetic interference [41]. Evaluations on both the thermocouple and the FBG sensor may help design and develop the new diffusing applicator tip equipped with a temperature feedback function.

According to Figure 3. 4, the definite deformation of a tissue lumen occurred after 10-*s* irradiation and commenced to achieve structural integrity. In spite of partial tissue collapse at the bottom (Figure 3. 4(b)), the 10-*s* irradiation vividly yielded circumferential tissue coagulation with a rather uniform thickness (0.9 ± 0.2 *mm*; Figure 3. 5). The light distribution skewed to the distal end (Figure 3. 1) could be responsible

for the lumen partially and inwardly filled with tissue at the bottom (Figure 3. 4(b)). In case of the shorter irradiation (5 s), the top part of the tissue lumen was coagulated primarily due to non-homogeneous light distribution, leading to the entire occlusion of the lumen after removal of a glass tube. Accordingly, the irradiation time was a critical factor to determine the minimum coagulation thickness for radial lumen expansion, given the testing conditions. As uneven light distribution resulted in non-uniform tissue deformation along with the prolonged coagulation, development of more cylindrical light emissions will be instrumental in rapidly and evenly achieving the luminal expansion with the minimal tissue denaturation. In fact, the complete formation of the coagulation barrier around the rim could obtain tissue integrity and dilate the tissue lumen. The ramification of the luminal expansion would thereby be to secure a larger channel for the obstructed tubular tissue due to stricture. However, the excessive generation of the denatured tissue often leads to collagenous fibrosis and eventually recurrence of stricture. Therefore, further *in vivo* studies will be performed to identify healing response of the esophageal tissue and the minimum tissue injury for minimizing fibrosis in the tissue after photothermal treatment.

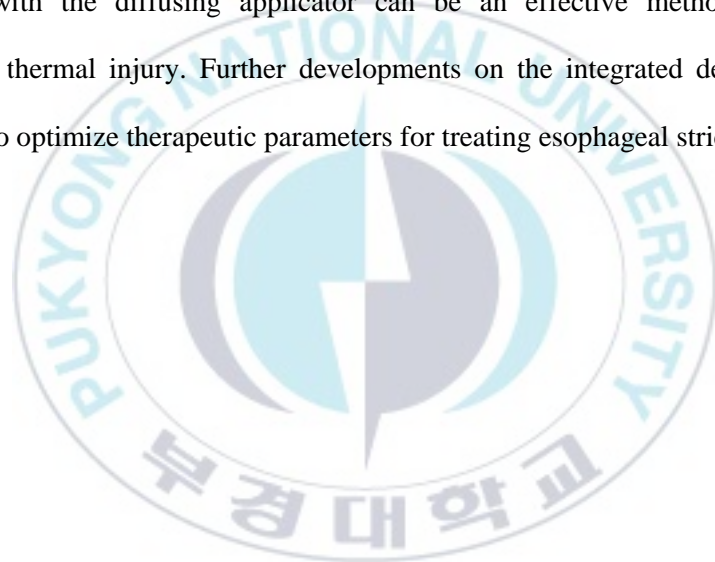
Application of an optical diffusing device demonstrated the potential luminal expansion by constantly maintaining the interstitial temperature during photothermal treatment. However, a glass tube was initially used to create a hole to mimic a lumen during the tests. In order to attain clinical applicability, a mechanical basket device is currently under development. Integration of the basket with the diffusing applicator

would thus be able to simultaneously coagulate and deform tubular tissue and to effectively expand the obstructed lumen. In addition, a thermocouple for temperature feedback can be readily attached to one of basket ribs without self-heating due to direct light absorption. *In vivo* rabbit models of esophageal stricture were recently developed to evaluate therapeutic outcomes. In turn, the *in vivo* tissue responses will be examined to identify the optimal treatment parameters such as power, irradiation time, and pulse mode for stricture treatment. Acute tissue testing will be performed to define the immediate inflammatory responses, the extent of basket expansion (force and length) for luminal passage, and the minimum coagulation depth for necrosis. Chronic testing (1~2 months) will also be conducted to evaluate the long-term wound healing responses, the recurrence rate of esophageal stricture, and the rate of changes in the lumen area after the thermal treatment.



3.6 Conclusion

A temperature feedback controller was implemented to achieve effective photothermal treatment for tissue dilation. Due to cylindrical light distribution, a diffusing applicator entailed circumferential temperature elevations during photocoagulation of tubular tissue. Effective dilation of the tubular tissue may require the minimum thickness of tissue denaturation. Integration of the temperature feedback controller with the diffusing applicator can be an effective method to reduce undesirable thermal injury. Further developments on the integrated device will be conducted to optimize therapeutic parameters for treating esophageal stricture.



Chapter 4: Summary

In the present study, the feasibility of a balloon catheter integrated with an optical diffusing fiber and the application to minimize undesired thermal injury was confirmed by ex vivo test. Both mechanical dilation and light diffusion were contributed to expand the lumen of the bile duct accompanying uniform coagulative necrosis. The balloon catheter-integrated diffusing applicator may be a feasible therapeutic device for treating tubular tissue structures in an effective manner. Integration of the temperature feedback controller with the diffusing applicator can be an effective method to reduce undesirable thermal injury. For the future study, more efforts are still need to develop the balloon catheter integrated with an optical diffusing applicator and optimize the parameters to improve predictability for the efficacy photothermal treatment with mechanical dilation.

References

1. Ahtaridis, G., W.J. Snape Jr, and S. Cohen, *Clinical and manometric findings in benign peptic strictures of the esophagus*. Digestive diseases and sciences, 1979. **24**(11): p. 858-861.
2. Lawson, J.D., et al., *Frequency of esophageal stenosis after simultaneous modulated accelerated radiation therapy and chemotherapy for head and neck cancer*. American journal of otolaryngology, 2008. **29**(1): p. 13-19.
3. Chen, A.M., et al., *Late esophageal toxicity after radiation therapy for head and neck cancer*. Head & neck, 2010. **32**(2): p. 178-183.
4. Pace, F., S. Antinori, and A. Repici, *What is new in esophageal injury (infection, drug-induced, caustic, stricture, perforation)? Current opinion in gastroenterology*, 2009. **25**(4): p. 372-379.
5. Zografos, G., et al., *Drug-induced esophagitis*. Diseases of the Esophagus, 2009. **22**(8): p. 633-637.
6. Ono, S., et al., *Predictors of postoperative stricture after esophageal endoscopic submucosal dissection for superficial squamous cell neoplasms*. Endoscopy, 2009. **41**(8): p. 661.
7. Dadhwal, U. and V. Kumar, *Benign bile duct strictures*. medical journal armed forces india, 2012. **68**(3): p. 299-303.
8. Foutch, P.G. and M.V. Sivak Jr, *Therapeutic endoscopic balloon dilatation of the extrahepatic biliary ducts*. American Journal of Gastroenterology, 1985. **80**(7).
9. Draganov, P., et al., *Long-term outcome in patients with benign biliary strictures treated endoscopically with multiple stents*. Gastrointestinal endoscopy, 2002. **55**(6): p. 680-686.
10. Nguyen, T.H., et al., *Circumferential irradiation for interstitial coagulation of urethral stricture*. Optics express, 2015. **23**(16): p. 20829-20840.
11. Smith, M., S. Sherman, and G. Lehman, *Endoscopic management of benign strictures of the biliary tree*. Endoscopy, 1995. **27**(03): p. 253-266.
12. Katabathina, V.S., et al., *Adult bile duct strictures: role of MR imaging and MR cholangiopancreatography in characterization*. Radiographics, 2014. **34**(3): p. 565-586.
13. Hastier, P., et al., *Long term treatment of biliary stricture due to chronic pancreatitis with a metallic stent*. The American journal of gastroenterology, 1999. **94**(7): p. 1947.

14. Vallon, A., et al., *Endoscopic retrograde cholangiography in post-operative bile duct strictures*. The British journal of radiology, 1982. **55**(649): p. 32-35.
15. Davids, P.H., et al., *Randomised trial of self-expanding metal stents versus polyethylene stents for distal malignant biliary obstruction*. The Lancet, 1992. **340**(8834-8835): p. 1488-1492.
16. Knyrim, K., et al., *A prospective, randomized, controlled trial of metal stents for malignant obstruction of the common bile duct*. Endoscopy, 1993. **25**(03): p. 207-212.
17. Costamagna, G. and I. Boškoski, *Current treatment of benign biliary strictures*. Annals of Gastroenterology: Quarterly Publication of the Hellenic Society of Gastroenterology, 2013. **26**(1): p. 37.
18. Ahn, M., et al., *Endoluminal application of glass-capped diffuser for ex vivo endovenous photocoagulation*. Journal of biophotonics, 2017. **10**(8): p. 997-1007.
19. Spears, J.R., *Percutaneous transluminal coronary angioplasty restenosis: potential prevention with laser balloon angioplasty*. American Journal of Cardiology, 1987. **60**(3): p. 61-64.
20. Reis, G.J., et al., *Laser balloon angioplasty: clinical, angiographic and histologic results*. Journal of the American College of Cardiology, 1991. **18**(1): p. 193-202.
21. Nguyen, T.H., et al., *Temperature feedback-controlled photothermal treatment with diffusing applicator: theoretical and experimental evaluations*. Biomedical optics express, 2016. **7**(5): p. 1932-1947.
22. Cox, B., *Introduction to laser-tissue interactions*. PHAS, 2007. **4886**: p. 1-61.
23. Kang, H.W., J. Kim, and J. Oh, *Enhanced photocoagulation with catheter-based diffusing optical device*. Journal of biomedical optics, 2012. **17**(11): p. 118001-118001.
24. Kwon, J., et al., *Computational analysis of endometrial photocoagulation with diffusing optical device*. Biomedical optics express, 2013. **4**(11): p. 2450-2462.
25. Aslan, N. and Y. Cebeci, *Application of Box-Behnken design and response surface methodology for modeling of some Turkish coals*. Fuel, 2007. **86**(1-2): p. 90-97.
26. Sassoli, C., et al., *Low intensity 635 nm diode laser irradiation inhibits fibroblast-myofibroblast transition reducing TRPC1 channel expression/activity: New perspectives for tissue fibrosis treatment*. Lasers in surgery and medicine, 2015.

27. Richter, J.E., *Long-term management of gastroesophageal reflux disease and its complications*. American Journal of Gastroenterology, 1997. **92**.
28. Marks, R. and M. Shukla, *Diagnosis and management of peptic esophageal strictures*. The Gastroenterologist, 1996. **4**(4): p. 223-237.
29. Kirsch, M., et al., *Intralesional steroid injections for peptic esophageal strictures*. Gastrointestinal endoscopy, 1991. **37**(2): p. 180-182.
30. Song, H.-Y., et al., *Covered Retrievable Expandable Nitinol Stents in Patients with Benign Esophageal Strictures: Initial Experience I*. Radiology, 2000. **217**(2): p. 551-557.
31. McLean, G., et al., *Radiologically guided balloon dilation of gastrointestinal strictures. Part II. Results of long-term follow-up*. Radiology, 1987. **165**(1): p. 41-43.
32. Wesdorp, I., et al., *Results of conservative treatment of benign esophageal strictures: a follow-up study in 100 patients*. Gastroenterology, 1982. **82**(3): p. 487-493.
33. Patterson, D.J., et al., *Natural history of benign esophageal stricture treated by dilatation*. Gastroenterology, 1983. **85**(2): p. 346-350.
34. Starck, E., et al., *Esophageal stenosis: treatment with balloon catheters*. Radiology, 1984. **153**(3): p. 637-640.
35. Radecke, K., G. Gerken, and U. Treichel, *Impact of a self-expanding, plastic esophageal stent on various esophageal stenoses, fistulas, and leakages: a single-center experience in 39 patients*. Gastrointestinal endoscopy, 2005. **61**(7): p. 812-818.
36. Masters, A., et al., *Interstitial laser hyperthermia: a new approach for treating liver metastases*. British journal of cancer, 1992. **66**(3): p. 518.
37. Mack, M., et al., *Percutaneous MR imaging-guided laser-induced thermotherapy of hepatic metastases*. Abdominal imaging, 2001. **26**(4): p. 369-374.
38. Gowda, A., et al., *Light diffusing tip*. 2007, Google Patents.
39. Stokbroekx, T., et al., *Commonly used fiber tips in endovenous laser ablation (EVLA): an analysis of technical differences*. Lasers in medical science, 2014. **29**(2): p. 501-507.
40. Vesselov, L.M., W. Whittington, and L. Lilge, *Performance evaluation of cylindrical fiber optic light diffusers for biomedical applications*. Lasers in surgery and medicine, 2004. **34**(4): p. 348-351.

41. Jonghun, L., ? *Characteristics of Fiber Bragg Grating Temperature Sensor using Thermal Strain of an External Tube*. *Journal of Korean Physical Society*, 2011. **59**: p. 3188.



Acknowledgments

Graduate school was incontrovertibly my most important life experience thus far. Both the outstanding academic experience, the professional and social interactions with other incredible and diverse research groups had reformed me as scientist and as a person. I would like to acknowledge and sincerely thank all of the people who have helped make this thesis possible, particularly:

I would like to express my deep and sincere gratitude to my supervisor, Professor Hyun Wook Kang who first brought me into the world of research and whom I began to learn about laser tissue interaction, optical system and Biomedical Engineering. His encouragement, enthusiasm and perpetual demand for excellence have been inspirational throughout my work. In addition, he always gives many in-depth discussion about results, and willing to help his students with their research.

I would like to thank Van Nam Tran, Van Gia Truong, Kim Hyejin, Hwang Jieun, Yeachan Lee, Hanjae Pyo and the other member of Bio-Ablation Lab who as good friends, was always give me best suggestions. Special thanks to Prof. Jung Hwan Oh and Prof. Sung-Won Kim, who were willing to participate in my final defense committee.

This research was supported by a grant of the Korea Health Technology R&D Project through the Korea Health Industry Development Institute (KHIDI), funded by the Ministry of Health & Welfare, Republic of Korea (grant number: HI16C1017).